

## **Determining the specific heat capacity and thermal conductivity for adjusting boundary conditions of FEM model**

A. Kešner<sup>1,\*</sup>, R. Chotěborský<sup>1</sup> and M. Linda<sup>2</sup>

<sup>1</sup>Department of Material Science and Manufacturing Technology Faculty of Engineering, Czech University of Life Sciences Prague, Kamýcká 129, CZ165 21 Prague – Suchbát, Czech Republic

<sup>2</sup>Department of Electrical Engineering and Automation, Faculty of Engineering, Czech University of Life Sciences Prague, Kamýcká 129, CZ165 21 Prague – Suchbát, Czech Republic

\*Correspondence: kesner@tf.czu.cz

**Abstract:** One of modern way of the heat treatment process of agricultural tools such as chisels or tines is FEM modelling. FEM models needs the accurate boundary conditions for successful solution. Specific heat capacity and thermal conductivity are important parameters for the design of the physical properties of heat treatment. These parameters are used for the formation of the temperature field during the cooling process at the heat treatment. More accurate parameters allow you to better estimate the final microstructure in the entire cross-section of the material. Specific heat capacity and thermal conductivity are known from material sheets, but they are stated as constant values. This is the reason why this work is focused on the determination of specific heat capacity and thermal conductivity of steel during the quenching. For the experiment in this work was chosen material 25CrMo4. The values of specific heat capacity and thermal conductivity were determined by comparing the experimentally measured cooling curves and cooling curves generated by the mathematical model. The dependences of specific heat capacity and thermal conductivity were compared in temperature, so that the relationships of cooling curves were statistically significant under alfa level 0.05.

**Key words:** specific heat capacity, thermal conductivity, FEM model, quenching.

### **INTRODUCTION**

Mechanical properties and production efficiency are important aspects in the production of agricultural tools. Combining these requirements need a correct preparation of production as the correct selection of materials including heat treatment. The simulation of heat treatment can be designed by FEM models nowadays allows. FEM models shown good prediction of microstructure, mechanical properties and deformation of the material (Rabin et al., 2013).

Bainitic structure or combination of bainitic and martensitic structures are suitable for agricultural tools. (Narayanaswamy et al., 2016a; Narayanaswamy et al., 2016b). The boundary conditions of FEM models is necessary set to accuracy model with respect to microstructure phases. It can be determined by experiments for evaluation of heat flux between steel and quenching media. (Kesner 2015; Chotěborský & Linda 2015b), also

chemical composition of steels, specific heat capacity  $c_p$  and thermal conductivity  $\lambda$  must be set with the highest possible accuracy. Specific heat capacity and thermal conductivity during the heat treatment show different values. Phase transformations during the heat treatment depend on physical properties of the material. When the cooling rate increases, the diffusive process is interrupted causing a change in the metallurgical microstructure which will affect steel properties (Lara-Guevara et al., 2016).

Size of the specific heat capacities and thermal conductivities reported at room temperature is dependent on the condition of heat treatment. Technical literatures are not given information about dependency between microstructure of steel and physical properties. A higher thermal conductivity reduces temperature gradients at the surface of a tool. A high thermal conductivity is beneficial for hardening because determines the cooling rate of a metal blank from the austenitization temperature and thereby directly influences cycle time and productivity (Kessler & Reich, 2009; Wilzer et al., 2013). The thermal diffusivity and the thermal conductivity decreased as the carbon content increased (Lara-Guevara et al., 2016).

Thermal conductivity and specific heat capacity are increases with increasing carbon content (Lara-Guevara et al., 2016).

Specific heat capacity and thermal conductivity are obtained: using photoacoustic techniques and thermal relaxation (Kessler & Reich, 2009), generating regression analysis, a simple extrapolation of data (Kuepferle et al., 2015) or deriving by calculation from electrical resistance depending on temperature (Rabin et al., 2013).

The aim of this work is to determination of physical properties of material like specific heat capacity and thermal conductivity for FEM models of agriculture tools. Physical properties of material were determined by algorithm where we compared experimental data with model.

## MATERIAL AND METHODS

Specific heat capacity and thermal conductivity was determined for the material 25CrMo4. The chemical composition of the material used is shown in Table 1.

**Table 1.** Chemical composition of steel 25CrMo4 in wt. %

	C	Mn	Si	P	S	Cr	Ni	Mo	Cu	V
25CrMo4	0.250	0.710	0.230	0.018	0.022	1.030	0.090	0.210	0.230	0.004

Specific heat capacity and thermal conductivity was determined using FEM model. Heat flux was measured during cooling. The results of heat flow were used for comparison of experimentally measured curves and cooling curves.

Some authors (Kesner, 2015) have been described measuring of heat flux. Samples ( $\varnothing 25\text{--}50$  mm) were heated at temperatures 800, 900 and 1,000 °C for 30 minutes. Water was used as the quenching media. Cooling time lasted until cool the sample throughout the volume (water has 20 °C). Sample cooling was repeated three times for each measured sample. Dependency of heat flux on absolute temperature was transformed to relative temperature (dimensionless temperature-from 0 to 1). Iterative method algorithm of solution was used for the calculation of heat capacity and thermal conductivity. SCILAB 5.5.1. was used to compilation the algorithm – see Fig. 1.

Neumann boundary condition heat flux used for iterative calculation (Telejko 2004; Chotěborský & Linda 2015a).

Heat flux was determined from the measured temperatures for the constant  $c_p$  and  $\lambda$ , settings data included boundary conditions (heat flux) and material characteristic (nonstationary  $c_p$  and  $\lambda$ ). The next step was run FEM model. Comparison measured and modeled temperature field and determination of sum of error temperature. Last step was setting new  $c_p$  and  $\lambda$ . After full iteration the file sum of error was evaluated and minimal sum of errors was found.

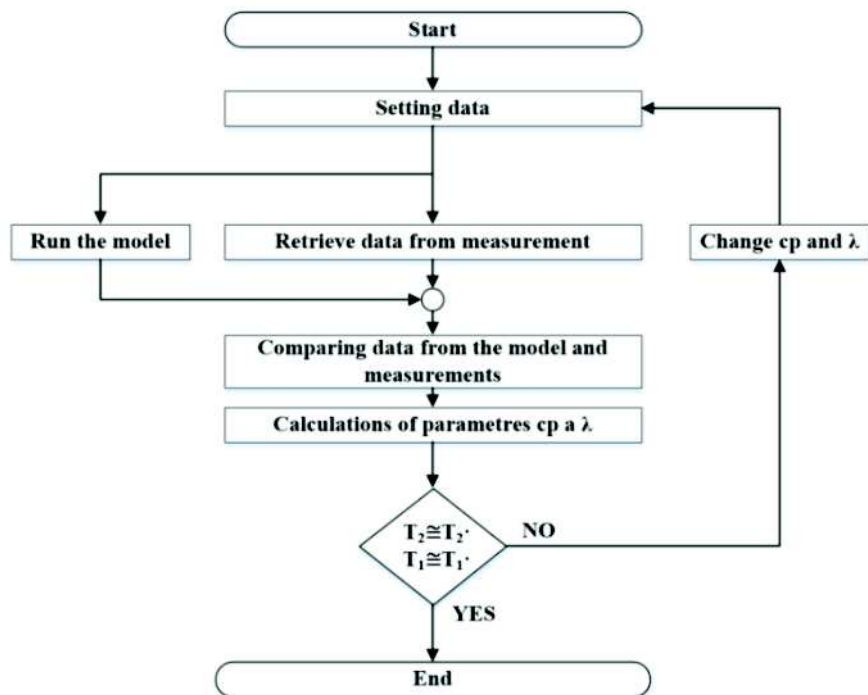


**Figure 1.** Algorithm for finding the smallest difference between calculated and measured temperatures field.  $T_1$  and  $T_2$  are measured temperatures,  $T_1$  and  $T_2$  are modeled temperatures.

Iterations were assembled into the matrix. Each iteration included a combination of values of specific heat capacity and thermal conductivity. Relative temperatures were assigned to each value (in table labeled  $c_0$  – constant of boost,  $c_{sop}$ ,  $c_1$  – constants of slope from the peak) of the specific heat capacity and thermal conductivity. The range of values is shown in the Table 2. The first row contains the smallest set value and the last row of the highest set value. Heat capacity and thermal conductivity were found in the material sheet 25CrMo4 for a constant temperature at 20 °C ( $\lambda = 46.44 \text{ W m}^{-1} \text{ K}^{-1}$ ,  $c_p = 590 \text{ J kg}^{-1} \text{ K}^{-1}$ ). Step 0.05 was used to shift the relative temperature (in places where it counts a given size thermal conductivity and heat capacity). The algorithm was designed for calculating and comparing iterations. The values were loaded from the first iteration. Cooling curves were calculated for the core and the surface. Heat equation was used to calculate (Eq. 1).

$$\frac{\partial}{\partial x} \left( \lambda \frac{\partial T}{\partial x} \right) + \frac{\partial}{\partial y} \left( \lambda \frac{\partial T}{\partial y} \right) + \frac{\partial}{\partial z} \left( \lambda \frac{\partial T}{\partial z} \right) + Q = \rho \times c_p \times \frac{\partial T}{\partial t} \quad (1)$$

$\lambda$  – thermal conductivity,  $Q$  – is the inner heat-generation rate per unit volume,  $T$  – temperature,  $\rho$  – density,  $c_p$  – heat capacity,  $t$  – time.

Calculation began by thermal conductivity, which has a high sensitivity to the temperature cooling rate. The procedure was run for all iterations. Cooling curves, which were experimentally measured, they were also loaded to algorithm. The calculated and experimentally measured cooling curve were compared after simulation. The differences between the calculated and experimentally measured curves were compared. The smallest difference between measured and calculated values of temperature is closest to the fair value of specific heat capacity and thermal conductivity. Iterations are calculated for the cooling time up to 30 seconds, which is the high heat transfer from the the material and the phase transformation.

Newton polynomials were used to calculate (Eq. 2). Triangular matrix is composed of iterations (Eq. 3).

$$n_j(x) := \prod_{i=0}^{j-1} (x - x_i) \quad (2)$$

$$\begin{bmatrix} 1 & & & 0 \\ x_1 - x_0 & & & 1 \\ x_1 - x_0 (x_1 - x_0) & (x_1 - x_0) & & 2 \end{bmatrix} \quad (3)$$

For the calculation was used software Windows 7 Enterprise, Intel® Xeon® Processor CPU E5 – 1650 v3@, processor base frequency 3.50 GHz.

**Table 2.** Combinations of iterations for calculating the heat capacity and thermal conductivity

Shift of point	Thermal conductivity			Shift of point	Heat capacity		
	$c_0$	$c_{sop}$	$c_1$		$c_0$	$c_{sop}$	$c_1$
0.35	20	37.5	20	0.35	1,150	750	1,050
0.4	20	37.5	20	0.35	1,150	750	1,050
.	.	.	.	.	.	.	.
.	.	.	.	.	.	.	.
.	.	.	.	.	.	.	.
0.4	25	42.5	25	0.45	1,250	850	1,150
0.45	25	42.5	25	0.45	1,250	850	1,150

## RESULTS AND DISCUSSION

Dependence between the sum of errors and iterations temperature is shown in Fig. 2. The differences (errors) of temperatures were calculated and compared separately for core and separately for the sample surface. The differences in core temperature and surface were added up for each iteration.

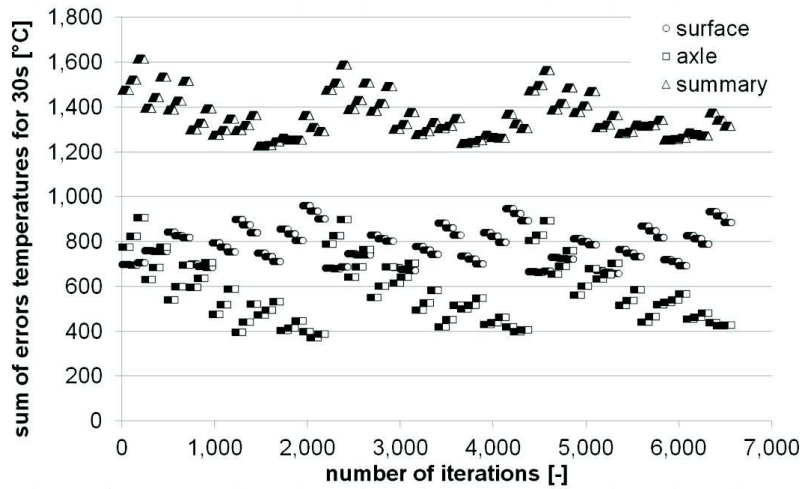


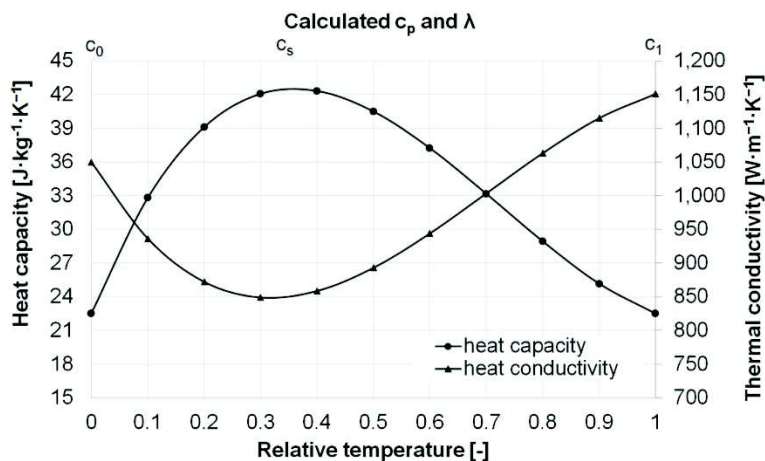
**Figure 2.** Dependency between sum of errors temperatures.

The smallest difference sum of the temperature was found to closest to the real values of thermal capacity and thermal conductivity. The smallest difference sum of temperature was detected for the iteration which is shown in Table 3.

**Table 3.** Iteration for the smallest difference sum of temperature

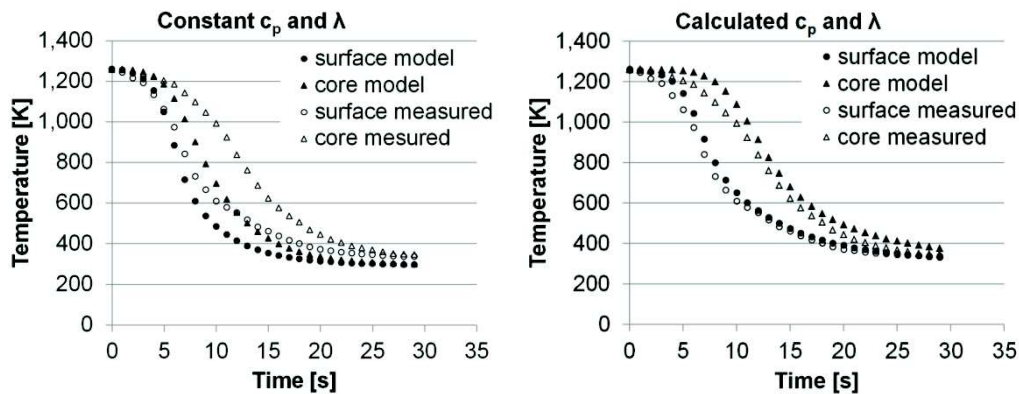
Shift of point	Thermal conductivity			Shift of point	Heat capacity		
	$c_0$	$c_{sop}$	$c_1$		$c_0$	$c_{sop}$	$c_1$
0.4	22.5	42.5	22.5	0.35	1,150	850	1,050

Table 3 show the values of specific heat capacity and thermal conductivity at a given relative temperature which is closest to real values. Fig. 3 shows the course of the thermal capacity and thermal conductivity depending on the relative temperature.



**Figure 3.** The dependence of the heat capacity and thermal conductivity to relative temperature differential for the smallest experimentally measured and calculated temperatures.

Values  $c_p$  and  $\lambda$  can be application in the FEM model, which can be used for a simulation of the thermal treatment of the material 25CrMo4. FEM model was created for simulation with the size of the thermal capacity and thermal conductivity at a given temperature. The advantage is more precise simulation of heat treatment than if they had entered constant the value from the material sheets – see Fig. 4.



**Figure 4.** Left side: cooling curves for stationary  $c_p$  and  $\lambda$  in FEM model, right side: cooling curves for nonstationary  $c_p$  and  $\lambda$  in FEM model.

The procedure is relatively time demanding for software. Processor total time was 336 hours for all iterations. Processor time could be reduced by better choice matrix iterations. Iteration could be adjusted by using the adaptive testing algorithm. The program would be assembled with the value of the exact error. The algorithm would not calculate all steps, but only steps with the smallest error until the set conditions. The number of steps is not known with these settings iteration. Large differences between the actual data and calculated data can be adjusted refining steps. Bigger time for calculation and memory software is required for this procedure.

(Prasanna Kumar, 2013) in their work indicates that the accuracy of calculations based on the finite element method depends on the discretization and the time step. Effect of errors has been studied in setting a time step of 0.1 and 0.5 seconds to simulate hardening material C45. The error for time step 0.1 seconds was below 0.50%. The error for time step 0.5 seconds was below 2.25%. The errors were compared with experimentally measured data. Calculations for time step 0.1 seconds were CPU intensive, error for time step 0.5 seconds is considered acceptable.

(Teixeira et al. 2009) shows the heat capacity and thermal conductivity depending on the temperature. The course of thermal conductivity and heat capacity are characterized by at least five points. But we were given three points in this work. More points have higher demands on the software, respectively processor time for calculates. More iterations or choosing a larger time step should be done. Choosing a larger time step could increased again error.

(Wang et al., 2008) in their work compares experimentally calculated and measured temperature during cooling. Cooling was calculated for the constant and variable thermal conductivity and heat capacity. Their results indicate that the variable thermal conductivity and heat capacity values approaching to the experimentally measured data.

## CONCLUSIONS

The following findings can be summarized from the calculations this work:

- Thermal conductivity and heat capacity dependency on the temperature can be calculated by the procedure describe in this work.
- The values of the heat capacity and thermal conductivity dependency on the relative temperature may be used to heat equation FEM model. The algorithm will be more accurate than if we used algorithm without constant values heat capacity and thermal conductivity.
- The smallest difference between the temperatures measured and modeled (for variables  $c_p$  and  $\lambda$ ). The smallest difference value (suma error of temperatures for core and surface) was calculated as 1,224 °C for 30 seconds from the start of cooling.
- Processor total time used in this work was 336 hours for all iterations. A shorter time could be achieved by a better choice of iterations for modelling the variable  $c_p$  and  $\lambda$ .

ACKNOWLEDGEMENTS. Supported by Internal grant 31140/1312/3108 agency of Faculty of Engineering, Czech University of Life Sciences in Prague

## REFERENCES

- Chotěborský, R. & Linda, M. 2015a. FEM based numerical simulation for heat treatment of the agricultural tools. *Agronomy Research* **13**(3), pp.629–638.
- Chotěborský, R. & Linda, M. 2015b. Prediction Of Mechanical Properties Of Quench Hardening Steel. *Scientia Agriculturae Bohemica* **46**(1), 26–32.
- Kesner, A. 2015. Determination of the heat flux for FEM models (Stanovení tepelného toku pro MKP modely). In International Scientific Conference of Young in Zvolen 2015, 67–75.
- Kessler, O. & Reich, M. 2009. Similarities and differences in heat treatment simulation of aluminium alloys and steels. *Materialwissenschaft und Werkstofftechnik* **40**(5–6), 473–478.
- Kuepferle, J., Wilzer, J., Weber, S. & Theisen, W. 2015. Thermo-physical properties of heat-treatable steels in the temperature range relevant for hot-stamping applications. *Journal of Materials Science* **50**(6), 2594–2604.
- Lara-Guevara, A., Ortiz-Echeverri, C.J., Rojas-Rodriquez, I., Mosquera-Mosquera, J.C., Ariza-Calderón, H., Ayala-Garcia, I. & Rodriguez-García, M.E. 2016. Microstructural, Structural, and Thermal Characterization of Annealed Carbon Steels. *International Journal of Thermophysics* **37**(10), p. 99.
- LIU, H. Song, Z.L., Cao, Q., Chen, S.P. & Meng, Q.S. 2016. Microstructure and Properties of Fe-Cr-C Hardfacing Alloys Reinforced with TiC-NbC. *Journal of Iron and Steel Research International* **23**(3), 276–280.
- Narayanaswamy, B., Hodgson, P., Timokhina, I. & Beladi, H. 2016. The Impact of Retained Austenite Characteristics on the Two-Body Abrasive Wear Behavior of Ultrahigh Strength Bainitic Steels. *Metallurgical and Materials Transactions A*, **47**(10), 4883–4895.
- Narayanaswamy, B., Hodgson, P. & Beladi, H. 2016. Comparisons of the two-body abrasive wear behaviour of four different ferrous microstructures with similar hardness levels. *Wear* **350–351**, 155–165.
- Prasanna Kumar, T.S. 2013. Influence of Steel Grade on Surface Cooling Rates and Heat Flux during Quenching. *Journal of Materials Engineering and Performance* **22**(7), 1848–1854.

- Rabin, B.H., Swank, W.D. & Wright, R.N. 2013. Thermophysical properties of Alloy 617 from 25 °C to 1000 °C. *Nuclear Engineering and Design* **262**, 72–80.
- Teixeira, M.G., Rincon, M.A. & Liu, I.-S. 2009. Numerical analysis of quenching – Heat conduction in metallic materials. *Applied Mathematical Modelling* **33**(5), 2464–2473.
- Telejko, T. 2004. Analysis of an inverse method of simultaneous determination of thermal conductivity and heat of phase transformation in steels. *Journal of Materials Processing Technology* **155–156**, 1317–1323.
- Wang, J., Gu, J., Shan, X., Hao, X., Chen, N. & Zhang, W. 2008. Numerical simulation of high pressure gas quenching of H13 steel. *Journal of Materials Processing Technology* **202**(1–3), 188–194.
- Wilzer, J., Lüdtkke, F., Weber, S. & Theisen, W. 2013. The influence of heat treatment and resulting microstructures on the thermophysical properties of martensitic steels. *Journal of Materials Science* **48**(24), 8483–8492.